Current Applied Physics xxx (2010) 1–5

Contents lists available at ScienceDirect

Current Applied Physics

journal homepage: www.elsevier.com/locate/cap

Preparing large-scale WO_3 nanowire-like structure for high sensitivity NH_3 gas sensor through a simple route

Nguyen Van Hieu [a,*], Vu Van Quang [a], Nguyen Duc Hoa [a,**], Dojin Kim [b,***]

[a] International Training Institute for Materials Science (ITIMS), Hanoi University of Science and Technology (HUST), Hanoi, Vietnam
[b] Department of Materials Science and Engineering, Chungnam National University, Daejeon, Republic of Korea

ARTICLE INFO

Article history:
Received 29 July 2010
Received in revised form
13 October 2010
Accepted 1 November 2010
Available online xxx

Keywords:
WO_3 nanowires
SWCNTs template
NH_3 sensors

ABSTRACT

The large-scale nanowire-like (NW) structure of tungsten oxide is synthesized by the deposition of tungsten metal on the substrate of porous single-wall carbon nanotubes (SWCNTs) film, followed by thermal oxidation process. The morphology and crystallinity of the synthesized materials are analyzed by SEM, TEM, XRD, and Raman spectroscopy. Results showed that tungsten oxide NWs deposited on SWCNTs have a porous structure with an average diameter of about 70 nm and a length of up to micrometers. The NH_3 gas-sensing properties of tungsten NWs were measured at different temperatures. A maximum response of 9.7–1500 ppm at 250 °C with rapid response and recovery times of 7 and 8 s are found, respectively. In addition, the gas sensing mechanism of fabricated NWs is also discussed in term of surface resistivity and barrier height model.

1. Introduction

Nanostructured tungsten oxide materials have received tremendous interest in recent years because of their great potential applications as gas sensors [1,2], field emission devices [3], and photocatalysts [4]. Nanostructured tungsten oxide based gas sensors have been used for detecting a variety of gases, such as NO_2, CO, H_2, SO_2, H_2, and NH_3 [1,2,5,6]. In particular, nanostructured tungsten oxides like nanorods [7] and nanowires [8] can be used as high sensitive gas sensors, which are unattainable by the conventional materials. Nanostructured tungsten oxide nanorods, nanowires, nanotubes, nanoflakes and nanodisks have been synthesized by using high temperature evaporation, precipitation, hydrothermal reaction, and electrochemical or template assisted methods [2]. However, those mentioned methods have some drawbacks in gas sensing devices fabrication, especially for mass production because they require multiples synthesis processes including of (i) growth of nanowires, (ii) collection of nanowires, (iii) dispersal of the nanowires on solution, and (iv) deposition or alignment of nanowires on patterned metal electrodes [9,10]. These techniques require the use of expensive equipments such as an electron-beam lithography, focus ion beam and sputtering system to fabricate the electrical contacts. These approaches also present a series of uncontrollable processes such as sonification and dispersal of nanowires on pre-fabricated electrodes. Recently, we developed a new method for synthesizing tin oxide nanowires for gas sensor applications using SWCNTs as templates [11]. The method features: (i) the versatility of metal choice for the nanowires structure; (ii) easy control of the diameters, and most importantly; (iii) high porosity in the ensemble structure.

In this study, we report on the synthesis and characterization of NH_3 gas sensing of tungsten oxide nanowires-like structure (NWs) synthesized using SWCNT as templates. These preparation processes are expected to have importance for the mass-production of other metal oxides NWs gas sensors and quick implementation of the gas sensing applications of metal oxides nanowires.

2. Experimental

The fabrication of WO_3 NWs structures was carried out by (i) growing porous SWNTs as templates; (ii) depositing tungsten; and (iii) oxidizing tungsten. Briefly, SWNTs were synthesized directly on a SiO_2/Si substrate located on the inside wall of the arc-discharge chamber [11]. The deposition of tungsten on this SWCNT substrate was carried out with a DC sputtering system, in which a 2-inch tungsten target (purity of 4N) was used. The deposition was performed at room temperature and an Ar working pressure of 2×10^{-3} Torr. The deposition power was controlled at 13 W and maintained for 3 min to achieve a film thickness of 100 nm on the plane. During the deposition, the substrate was rotated for uniform

* Corresponding author. No. 1, Dai Co Viet Road, Hanoi, Vietnam. Tel.: +84 4 38680787; fax: +84 4 38692963.
** Corresponding author.
*** Corresponding author.
E-mail addresses: hieu@itims.edu.vn (N.V. Hieu), ndhoa@itims.edu.vn (N.D. Hoa), dojin@cnu.ac.kr (D. Kim).

1567-1739/$ – see front matter © 2010 Elsevier B.V. All rights reserved.
doi:10.1016/j.cap.2010.11.002

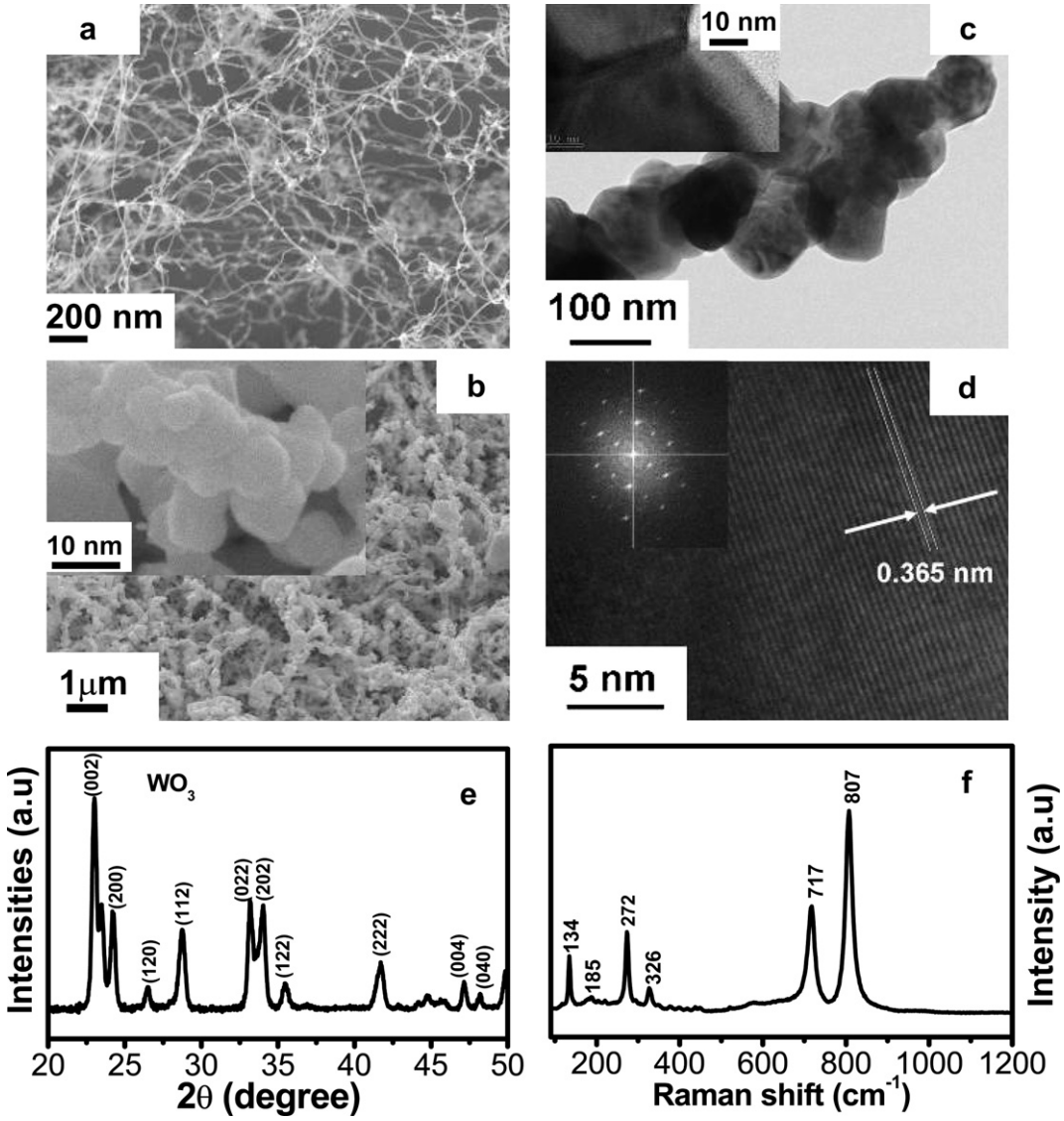

Fig. 1. Material characterizations; (a) FE-SEM image of SWCNTs templates; (b) FE-SEM image of WO_3 nanowires; (c) TEM image of single WO_3 nanowires; (d) High-resolution TEM lattice image and SAED pattern of WO_3 nanowires; (e) XRD pattern of WO_3 nanowires; and (f) the Raman spectra of WO_3 nanowires.

thickness. Through this method, NWs up to a wafer-scale were obtained. The oxidation of W was then carried out at temperatures of 700 °C in a tube furnace of atmospheric environment for 2 h. This temperature was high enough to totally burn out the SWCNT templates [11]. The synthesized materials were characterized by field emission scanning electron microscopy (FE-SEM, model JSM-7000F, JEOL), and field emission transmission electron microscopy (FE-TEM) (200 kV FE-TEM, model JEM-2100F, JEOL). The XRD measurements were carried out using CuKα-radiation (Model: D/max2500, Rigaku, Japan) to study the crystal structure and quality of the synthesized materials. The Raman spectra were also collected under ambient conditions using the 514.5 nm line of an argon–ion laser.

Gas sensing properties were studied by measuring the sensors with NH_3 (300–1500 ppm) at different temperatures (200–300 °C) using a homemade set-up with high-speed switching gas flow (from/to-air-to/from balance gas) and it presented detail in Ref. [12]. Balance gases (0.1% in air) were purchased from Air Liquid Group (Singapore). The system employed a flow-through with a constant rate of 300 sccm.

3. Results and discussion

The porous SWCNTs sample used in this work is shown in Fig. 1(a). The SWCNTs sample has high porosity without the impurity of carbon particles. These properties ensured that the NWs were obtained when SWCNTs were used as templates for tungsten oxide deposition. The FE-SEM image of the W-deposited SWCNTs is shown in Fig. 1(b). The deposition of tungsten did not destroy the porosity of the SWCNTs template. Because the structure of SWCNTs is stable during the bombardment of sputtered atoms, the tungsten atoms deposited on the surface of SWCNTs forms NWs, as in previous studies [13]. The tungsten NWs appear to be formed by an agglomeration of nanoparticles rather than by a continuous tube shape as shown by the inset in Fig. 1(b). This issue is one factor that enhances gas sensing properties of as-fabricated materials (this factor is discussed later in the paper). The tungsten oxide NWs have an average diameter of about 70 nm and variable lengths of up to several micronmeters (Fig. 1(c)). The diameter of the NWs is not completely homogenous but this issue is not essential for gas sensing application. Further characterization by HRTEM images

Please cite this article in press as: N.V. Hieu, et al., Preparing large-scale WO_3 nanowire-like structure for high sensitivity..., Current Applied Physics (2010), doi:10.1016/j.cap.2010.11.002

also confirms that the NWs are formed by the agglomeration of nanoparticles rather than by a continuous tube shape. The inset in Fig. 1(c) showed the grain boundary between two nanoparticles having different crystalline orientations. Each nanoparticle is a single crystal as revealed by the magnified HRTEM image (Fig. 1(d)), which shows clear lattice fringes with a distance of 0.36 nm belonging to the (200) plane of monoclinic WO_3. The single crystal of nanoparticles was also confirmed by the selective area electron diffraction (SAED) pattern illustrated in the inset of Fig. 1(d). The bright dots in the pattern indicate single crystallinity of WO_3.

Fig. 1(e) shows the XRD patterns of the synthesized WO_3 NWs after oxidation process. The peaks of XRD patterns can satisfactorily match with the documented diffraction pattern of monoclinic WO_3 (JCPDS card no. 43-1035). There is no diffraction peak of metallic tungsten indicating a complete oxidation at 700 °C.

Fig. 1(f) shows a typical Raman spectrum of WO_3 NWs where six well-resolved peaks can be observed (134, 185, 272, 326, 717 and 807 cm^{-1}). The comparison of Raman spectra recorded on the WO_3 NWs with those reported in the literature [14,15] suggested that they have the monoclinic phase and are formed by O–W–O microcrystalline clusters connected to each other by W–O–W bonds, with the terminal W–O bonds at the surface of the clusters. The peaks at 808 and 717 cm^{-1} are assigned as W–O–W stretching frequencies. The shorter W–O–W bonds are responsible for the stretching mode at 807 cm^{-1}, whereas the longer bonds are the source of the 717 cm^{-1} peak [15]. The peaks at 272 and 326 cm^{-1} can be ascribed to the W–O–W bending mode of the bridging oxygen, whereas those observed at 134 and 185 cm^{-1} are attributable to the lattice vibration of crystalline WO_3 [15].

To fabricate WO_3 NWs gas sensor, SiO_2/Si substrate was replaced by a SiO_2/Si substrate supported Pt comb-type electrodes, as illustrated in Fig. 2(a). Our fabrication method clearly provides a simple and controllable way of integrating NWs into gas sensing devices. In particular, this method can be used to fabricate the NWs gas sensors at wafer level scale, and is more straightforward than the recent reported method [16]. To investigate the NH_3 gas-sensing properties of WO_3 NWs, the NWs sensors were tested at different temperatures of 200, 250 and 300 °C to determine an optimized working temperature. Responses were measured with NH_3 gas at different concentrations of 300, 400, 500, 100 and 1500 ppm. The sensor response (R_{air}/R_{gas}) was plotted versus time as shown in Fig. 2(b–d), in which the vertical and horizontal axes were plotted in the same

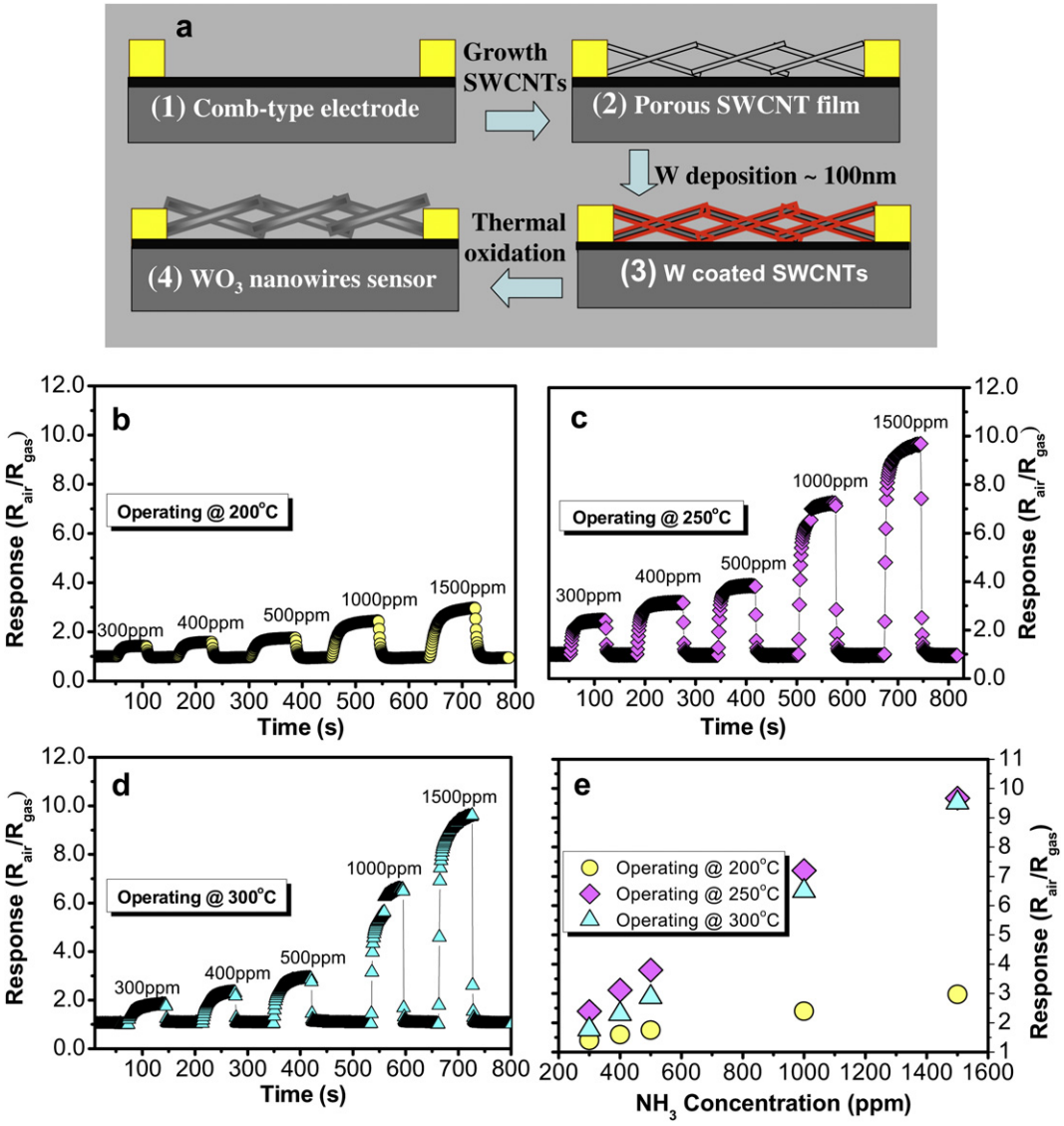

Fig. 2. NH_3 gas sensing characteristics (a) the gas sensor fabrication process; the sensor response to NH_3 gas at (b) 200 °C, (c)250 °C and (d) 300 °C; (e) the sensor response as function of NH_3 gas concentration.

Please cite this article in press as: N.V. Hieu, et al., Preparing large-scale WO_3 nanowire-like structure for high sensitivity..., Current Applied Physics (2010), doi:10.1016/j.cap.2010.11.002

scale. It can be seen that the temperature has an obvious influence on the response of sensors to NH_3 gas. The sensor exhibits a highest response at a working temperature of 250 °C, in which the responses are 2.39, 3.12, 3.80, 7.20, and 9.67 for 300, 400, 500, 1000, and 1500 ppm NH_3 concentration, respectively. The relationship between the sensor response and NH_3 gas concentration is summarized in Fig. 2(e). The response linearly increases as a function of NH_3 gas concentration in the measured range (from 300 ppm to 1500 ppm). Linear dependence of response and gas concentration is an advantage for designing read out signal circuits.

For practical applications, the response and recovery times of the gas sensors are highly important issues. Fig. 3 shows the plots of the dynamic responses at a tested temperature to 500 ppm NH_3 gas. The response time for gas exposure [$t_{90\%(air\text{-}to\text{-}gas)}$] and that for recovery [$t_{90\%(gas\text{-}to\text{-}air)}$] were calculated from the response-time data shown in Fig. 3. The $t_{90\%(air\text{-}to\text{-}gas)}$ values at operating temperature of 200, 250 and 300 °C are around 16, 7 and 15 s, respectively, whereas the $t_{90\%(gas\text{-}to\text{-}air)}$ values at operating temperature of 200, 250 and 300 °C are around 16, 8 and 13 s, respectively. Our WO_3 NWs sensors show relatively fast response and recovery times (about 10 s). These values are more significant if noticing that the response and recovery times reported by other researchers are in the range of from 1 min to 10 min [17]. In this work, we used high-speed switching gas chamber, detail was described in ref. [12]. The purge/filling time was about 3–5 s. Therefore, the rapid response and recovery of our sensors are due to the porosity of the NWs sensors and the use of high-speed switching gas chamber. Indeed, the porosity of NWs thin film enables gas molecules easily penetrate and adsorb on the surface of NWs, deceasing the response time. The high-speed switching gas chamber accelerates the purge/filling process and therefore decreases the response and recovery time.

Our WO_3 NW is formed from nanocrystallines linked together (see TEM images). Therefore, the gas sensing mechanism of our sensors can be explained by using surface resistivity and barrier height model as illustrated in Fig. 4. When n-type semiconducting tungsten oxide NWs are exposed to air, the oxygen molecules in air adsorb on the surface of WO_3 (in the form of O_2^-, O^-, or O^{2-}) [18] and withdraw electrons from NWs leading to the formation of an electron depletion layer [5]. The depth of the depletion layer (or space charge region) is estimated by the Debye-length $L = (\varepsilon\varepsilon_o k_B T/e^2 n_b)^{1/2}$, where n_b is the bulk carrier density, T is the absolute temperature, k_B is the Boltzmann constant, e is the electron charge, ε is the dielectric constant of WO_3, and ε_o is the dielectric permittivity of vacuum [6]. We could not measure the carrier density of our WO_3 NWs. However, we considered that the carrier density of WO_3 thin film fabricated by sputtering method is in the range of 4.0×10^{15}–4.0×10^{16} cm^{-3} [19]. Naturally, we cannot directly use this value as the carrier density for our WO_3 NWs because this value depends on the density of oxygen vacancies in the NWs. However, as a reference, the Debye-length calculated for temperature of 250 °C using $n_b = 4.0 \times 10^{15}$ cm^{-3} is about 11 nm, which is much smaller than the radius (35 nm) of WO_3 NWs. Therefore, the gas sensing mechanism of our WO_3 NWs obeys Shottky-barrier-controlled model [20]. Note that the WO_3 NW is formed from linked nanocrystallines; thus, the depletion layer generates an energy barrier at the boundary between nanocrystallines (Fig. 4). When exposed to ammonia gas, the NH_3 molecules interact with pre-adsorbed oxygen and release electrons to WO_3 NWs. The interaction of ammonium molecules and pre-adsorbed oxygen on the surface of WO_3 NWs is indicated in Eqs. (1)–(4):

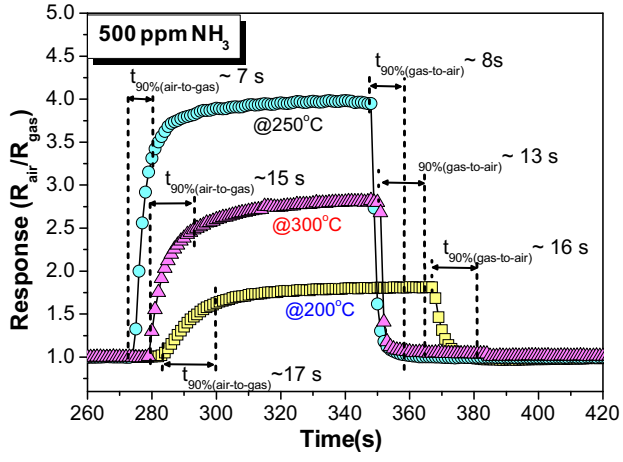

Fig. 3. The response transient of WO_3 NWs sensor to 500 ppm NH_3 gas for calculation of response-recovery time at operating temperatures of 200, 250 and 300 °C.

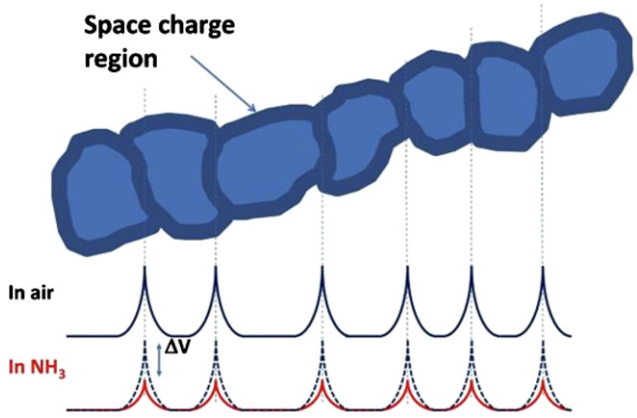

Fig. 4. The schematic illustration of gas sensing mechanism of WO_3 NWs.

$$NH_3(gas) \leftrightarrow NH_3(ads) \quad (1)$$

$$2NH_3(ads) + 3/2O_2^-(ads) \leftrightarrow N_2 + 3H_2O + 3e^- \quad (2)$$

$$2NH_3(ads) + 3O^-(ads) \leftrightarrow N_2 + 3H_2O + 3e^- \quad (3)$$

$$2NH_3(ads) + 3O^{2-}(ads) \leftrightarrow N_2 + 3H_2O + 6e^- \quad (4)$$

The free electrons released from Eqs. (1)–(4) increase the carrier in WO_3 NWs resulting in (i) a decrease in the surface resistivity of WO_3 NWs and (ii) a decrease in the barrier height ΔV_S at the boundary between nanocrystallines along the NW. The change in resistance due to the decrease in barrier height ΔV_S is described as $R_{gas} \sim R_{air}\exp(-e\Delta V_S/k_B T)$ [21]. According to the exponential function of ΔV_S the change in resistance (and response) is considerably more evident compared with others, suggesting that parameter (ii) is most likely the dominant parameter control in the sensing mechanisms of our NWs.

4. Conclusion

We have introduced a facile and scaleable method for synthesizing WO_3 NWs using SWCNTs as templates. The synthesized WO_3 NWs are smooth with single crystal but are formed from linked nanocrystallines. This nanowires structure is excellent for gas sensor application. The WO_3 NWs sensor shows very high response to NH_3 with fast response and recovery times (in seconds). The linear dependence of sensor response on NH_3 concentration in the measured range indicates promising potential for practical application. In addition, the sensing mechanism of the present WO_3 samples was discussed in the framework of surface resistivity and

Please cite this article in press as: N.V. Hieu, et al., Preparing large-scale WO_3 nanowire-like structure for high sensitivity..., Current Applied Physics (2010), doi:10.1016/j.cap.2010.11.002

barrier height, where the nanocrystallines boundaries were the dominant parameters those contribute on the sensing of NWs.

Acknowledgments

This work has been supported by the Vietnam's National Foundation for Science and Technology Development (NAFOSTED) for a Basic Research Project (No. 103.02.95.09).

References

[1] A. Ponzoni, E. Comini, G. Sberveglieri, J. Zhou, S.Z. Deng, N.S. Xu, Y. Ding, Z.L. Wang, Appl. Phys. Lett. 88 (2006) 203101.
[2] Z. Liu, M. Miyauchi, T. Yamazaki, Y. Shen, Sens. Actuator B. 140 (2009) 514.
[3] Q. Ya, W. Wu, J. Zhang, B. Liu, S.-S. Pei, Mater. Lett. 63 (2009) 2267.
[4] A. Abe, H. Takami, N. Murakami, B. Ohtani, J. Am, Chem. Soc. 130 (2008) 7780.
[5] G. Eranma, B.C. Joshi, D.P. Runthala, R.P. Gupta, Crit. Rev. Sol. Stat, Mater. Sci. 29 (2004) 111.
[6] Y.M. Zhao, Y.Q. Zhu, Sens. Actuators B. 137 (2009) 27.
[7] S. Piperno, M. Passacantando, S. Santucci, L. Lozzi, S. La Rosa, J. Appl. Phys. 101 (2007) 124504.
[8] S.Y. Kim, S.C. Ha, K. Kim, H. Yang, S.-Y. Choi, T.Y. Kim, Appl. Phys. Lett. 86 (2005) 213105.
[9] N.V. Hieu, Sens. Actuators B. 144 (2010) 425.
[10] E. Comini, C. Baratto, G. Faglia, M. Ferroni, A. Vomiero, G. Sberveglieri, Prog. Mater. Sci. 54 (2009) 1.
[11] N.D. Hoa, N.V. Quy, M.C. An, H.J. Song, Y.J. Kang, Y.S. Cho, D. Kim, J. Nanosci, Nanotech 8 (2008) 5586.
[12] N.V. Duy, N.V. Hieu, P.T. Huy, N.D. Chien, M. Thamilselvan, J. Yi, Physica E 41 (2008) 258.
[13] N.D. Hoa, N.V. Quy, Y.S. Cho, D.J. Kim, Sens. Actuators B. 135 (2009) 656.
[14] C. Bittencourt, R. Landers, E. Llobet, X. Correig, J. Calderer, Semicond. Sci. Technol. 17 (2002) 522.
[15] G.L. Frey, A. Rothschild, J. Sloan, R. Rosentsveig, R. Popovitz-Biro, R. Tenne, J. Solid State Chem. 162 (2001) 300.
[16] A. Vomiero, A. Ponzoni, E. Comini, M. Ferroni, G. Faglia, G. Sberveglieri, Nanotechnology 21 (2010) 145502.
[17] C.N. Xu, N. Miura, Y. Ishida, K. Matsuda, N. Yamazoe, Sens. Actuators B. 65 (2000) 163.
[18] H. Xia, Y. Wang, F. Kong, S. Wang, B. Zhu, X. Guo, J. Zhang, Y. Wang, S. Wu, Sens. Actuators B. 134 (2008) 133.
[19] M. DiGiulio, D. Manno, G. Micocci, A. Serra, A. Tepore, J. Phys. D: Appl.Phys. 30 (1997) 3211.
[20] O. Berger, T. Hoffmann, W.J. Fischer, J. Mater. Scie.: Mater. Electr. 15 (2004) 483.
[21] N.D. Hoa, N.V. Quy, D. Kim, Sens. Actuators B. 142 (2009) 253.

Please cite this article in press as: N.V. Hieu, et al., Preparing large-scale WO_3 nanowire-like structure for high sensitivity..., Current Applied Physics (2010), doi:10.1016/j.cap.2010.11.002